Anharmonicity and Universal Response of Linear Carbon Chain Mechanical Properties under Hydrostatic Pressure

Keshav Sharma,[1,*] Nathalia L. Costa,[2,*] Yoong Ahm Kim,[3] Hiroyuki Muramatsu,[4] Newton M. Barbosa Neto,[5,†] Luiz G. P. Martins,[6] Jing Kong,[7] Alexandre Rocha Paschoal,[2,‡] and Paulo T. Araujo[1,5,§]

[1]*Department of Physics and Astronomy, University of Alabama, Tuscaloosa, Alabama 35487, USA*
[2]*Department of Physics, Federal University of Ceara, 60455-760 Fortaleza, Ceara, Brazil*
[3]*Department of Polymer Engineering, School of Polymer Science and Engineering, and Alan G. MacDiarmid Energy Research Institute, Chonnam National University, 77 Yongbong-ro, Buk-gu, Gwangju 61186, Republic of Korea*
[4]*Research Institute for Supra-Materials, Shinshu University 4-17-1 Wakasato, Nagano, Japan*
[5]*Institute of Natural Sciences, Graduate Program in Physics, Federal University of Para, 66075-110 Belem, PA, Brazil*
[6]*Department of Physics, Massachusetts Institute of Technology, Cambridge, Massachusetts 02139, USA*
[7]*Department of Electrical Engineering and Computer Science, Massachusetts Institute of Technology, Cambridge, Massachusetts 02139, USA*

(Received 14 May 2020; accepted 23 July 2020; published 31 August 2020)

Isolated linear carbon chains (LCCs) encapsulated by multiwalled carbon nanotubes are studied under hydrostatic pressure (P) via resonance Raman scattering. The LCCs' spectroscopic signature C band around 1850 cm^{-1} softens linearly with increasing P. A simple anharmonic force-constant model not only describes such softening but also shows that the LCCs' Young's modulus (E), Grüneisen parameter (γ), and strain (ε) follow universal P^{-1} and P^2 laws, respectively. In particular, γ also presents a unified behavior for all LCCs. To the best of our knowledge, these are the first results reported on such isolated systems and the first work to explore universal P-dependent responses for LCCs' E, ε, and γ.

DOI: 10.1103/PhysRevLett.125.105501

Carbon is found in different sp^n ($n = 1$, 2, and 3) hybridizations [1–4] and extensive research on the mechanical properties in sp^3 (diamond) and sp^2 (graphene, graphite, and carbon nanotubes) materials is available in the literature [5–12]. Linear sp carbon chains have attracted much interest regarding its existence and stability [1,13–16]. Production of short carbon chains (8 to 28 atoms), known as polyynes, with alternate single and triple bonds ($\cdots - C \equiv C - C \equiv C - \cdots$) and end capping groups were one of the first systems to demonstrate the existence of stable linear carbon chains (LCCs) in the range of temperatures from 130 °C to 140 °C [17]. Later, Zhao *et al.* obtained stable LCCs (at ambient conditions) comprising ≈100 carbon atoms and encapsulated by multiwall carbon nanotubes (LCC@MWCNT) [18]. Since then, single- (SW), double- (DW), and MWCNT are considered ideal environments for fabricating stable LCCs with up to 6000 carbon atoms [3,19–22].

Hydrostatic pressure (P) Raman studies on the spectroscopic signatures of sp^2 materials such as CNTs (radial breathing mode, RBM, and G band), graphene (G- and 2D bands), and graphite (G- and 2D bands) have focused on the materials' mechanical, electronic, and vibrational properties as well as in the interactions between graphene sheets, concentric tubes in MWCNTs and/or bundled CNTs [7,10,11,23–26]. The spectroscopic signatures in these sp^2 materials undergo a frequency hardening with increasing P. However, little has been explored about the effect of P on LCCs' spectroscopic signature C band with frequencies (ω^0_{LCC}) around 1850 cm^{-1} at ambient conditions [27,28]. The literature has reported a ω_{LCC} softening with increasing P [27,28], in disagreement with the frequency hardening reported for RBM, G- and 2D bands in sp^2 materials. Coalescence of LCCs and charge transfer between chains and hosting tubes were hypothesized as the reason behind such C band softening but this topic is still an open question. Additionally, many theoretical works have reported values for the LCCs' Young's modulus ranging from 0.3 to 33 TPa [2,29,30]. These values span through a broad range and require more experiments, preferably in isolated systems, to be confirmed. Moreover, LCCs possess great technological appeal as one of the thinnest wires available for the next generation of ultracompact nanoelectronic and nanospintronic devices, and one-dimensional sensors whose performance depends on LCCs mechanical behaviors [30–34].

Here, we study the C band of four different LCC@MWCNT (or polyynes@MWCNT) submitted to pressures up to 4.60 GPa. We confirm the ω_{LCC} softening and propose a simple anharmonic force-constant model, based on the anharmonic nature of carbon-carbon (C-C) single bonds [32,35], that describes such softening and

 © 2020 American Physical Society

allows for obtaining pressure-dependent relations for the LCCs' Young's modulus (E), strain (ε), and Grüneisen parameter (γ). The model also explains very well results reported in the literature [27,28] [Supplemental Material (SM) [36]]. We show that E and γ follow a P^{-1} universal behavior, while ε follows a P^2 universal behavior. The model also shows asymptotic behaviors for E and γ, and the possibility for fine-tuning such parameters with increasing P. To the best of our knowledge, these are the first measurements exploring isolated LCC@MWCNT and their universal responses for E, ε and γ.

The LCC@MWCNT were synthesized using the arc discharge method described in a previous work [38]. Isolated LCCs@MWCNT (Fig. S1 in SM [36]) were obtained after sonication of as-grown LCC@MWCNT dispersed in acetone. The solution was then drop casted onto a silicon substrate equipped with horseshoe probes (70 μm diameter) [39]. Resonance Raman spectra (RRS) were acquired in a backscattering geometry using a 532 nm (2.33 eV) laser, a constant power density of 0.25 mW/μm^2 and a 50× objective (the LCCs' energy gaps are around 2.13 eV [36,38,40]). A membrane anvil diamond cell was used to apply the pressure loads [28,36,41]. Isolated MWCNTs [36,42,43] were characterized via atomic force microscopy and via resonance Raman spectra measurements (Fig. S1 in SM [36]). Comprehensive experimental details are available in SM [36]. Figure 1(a) shows the C band around 1850 cm^{-1} and a much weaker G band around 1575 cm^{-1}; the inset in Fig. 1(a) shows the C band's spectral evolution with P: ω_{LCC} decreases with increasing P. The C band for each isolated LCC@MWCNT shows four different LCCs [Fig. S1(c) in SM [36]] that continuously and reversibly evolves with distinct $d\omega_{\mathrm{LCC}}/dP$ [Figs. 1(b) and 1(c), and Fig. S2 and Table S1 in SM [36]]. At ambient conditions, the four LCCs are assigned to the Raman frequencies (±0.5 cm^{-1}) [Fig. S1(c) in SM [36]]: $\omega^0_{\mathrm{LCC}n_1} = 1848.4$ cm^{-1}, $\omega^0_{\mathrm{LCC}n_2} = 1853.0$ cm^{-1}, $\omega^0_{\mathrm{LCC}n_3} = 1856.6$ cm^{-1}, and $\omega^0_{\mathrm{LCC}n_4} = 1860.0$ cm^{-1}. The correlation between $\omega^0_{\mathrm{LCC}n_i}$ and n_i (number of carbon atoms for $i = 1, \ldots, 4$) is well addressed in the literature [1,36,38,40,44] which leads to LCCs with 36 to 41 carbon atoms [36].

Theoretical calculations have associated the ω_{LCC} behavior observed in Figs. 1(b) and 1(c) to coalescence [27] and charge transfer (CT) mechanisms [28]. These theoretical calculations considered that (1) coalescence would take place between LCCs in LCC@SWCNT [27]; and (2) charge transfer would take place between LCCs and inner tubes in LCC@DWCNT [28]. However, it is hard to reconcile why coalescence or charge transfer takes place only in LCC@SWCNT or LCC@DWCNT, respectively, but not on both. Moreover, these effects are associated with inner tubes' deformations and are predicted to efficiently happen for pressures beyond 9 GPa, which is twice the highest pressure in this work (for additional discussions, see [36]). For pressures below 9 GPa, the inner tubes remain essentially unaltered [45,46]. Therefore, the LCC@MWCNT's innermost tube deformation in the present work should be minimal [9,10,36,45–48]. We hypothesize, therefore, that the behavior of the LCC bonds associated with the anharmonic nature of C—C single bonds is the main phenomenon ruling our experiment [36].

Figure 1(b) shows that the variation of ω_{LCC} with increasing P from 0 to 4.60 GPa are associated with linear redshifts as large as 22 cm^{-1}. Linear blueshifts of the same order are observed with decreasing P (Fig. S2 in SM [36]), verifying that the experiment is reversible. The loading cycles show universal [i.e., $\omega_{\mathrm{LCC}}(P) \propto P$] but nonunified decrease rates (i.e., distinct $d\omega/dP$) for the ω_{LCC} softening, see Fig. 1(c) and Table S1 in SM [36]. As mentioned earlier, under hydrostatic pressure one would expect a harmonic hardening (softening) of the C—C bonds with increasing (decreasing) pressure, which in turn would lead to a positive (negative) $d\omega/dP$. For the LCCs studied here, however, the C—C bond seems to soften (harden) with increasing (decreasing) P (Fig. S2 in SM [36]). In our model, the harmonic C band frequency ω^0_{LCC} is given by [32,36]:

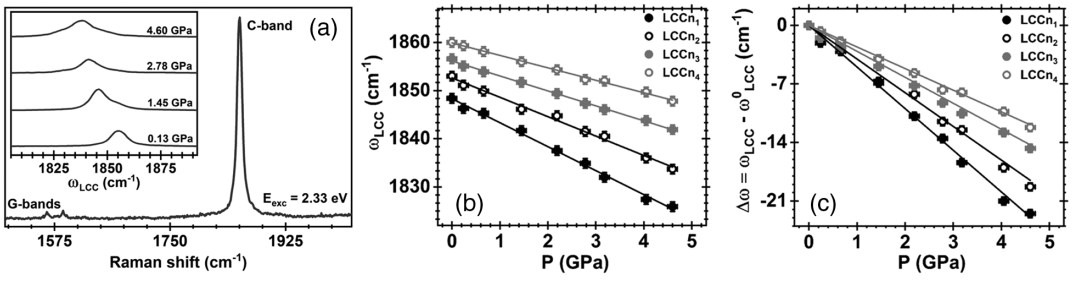

FIG. 1. (a) Resonance Raman profile of an isolated LCC@MWCNT. The G band is located around 1575 cm^{-1} and the C band is located around 1850 cm^{-1}. Inset: Representative spectra showing the evolution of the LCCs' C bands with P. (b) The C band Raman frequencies evolution $\omega_{\mathrm{LCC}n_1}$, $\omega_{\mathrm{LCC}n_2}$, $\omega_{\mathrm{LCC}n_3}$, and $\omega_{\mathrm{LCC}n_4}$ with P. The frequencies linearly decrease with distinct $d\omega_{\mathrm{LCC}}/dP$. (c) $\Delta\omega = \omega_{\mathrm{LCC}} - \omega^0_{\mathrm{LCC}}$ as a function of P: the loading cycles show a universal but nonunified $d\omega_{\mathrm{LCC}}/dP$.

$$\omega_{\mathrm{LCC}}^{0}=\sqrt{\frac{2[\mathrm{C}_1^0+\mathrm{C}_3^0]}{m}}, \tag{1}$$

where C_1^0 and C_3^0 are the corresponding effective force constants, at ambient pressure, for single and triple bonds, respectively, and m is the carbon atom mass. When the linear chains are submitted to external P, both the triple and single bonds are deformed. The triple bonds are considerably stiffer than the single bonds (about 167% stiffer) [32]. Thus, we consider that pressure-dependent alterations in the triple bonds (represented by C_3) are a minor contribution to the frequency's changes when compared to the pressure-dependent alterations in the single bonds (represented by C_1). Indeed, it is known that C_1 behaves anharmonically, while C_3 remains essentially harmonic [32,35]: as P increases, the carbon atoms connected by C_1 get close enough to experience a repulsive potential energy that is sufficiently strong to compete with the attractive potential making anharmonic contributions important to the net potential [32,35,49]. In fact, theoretical calculations have shown that LCCs will be in the anharmonic regime for pressures above 0.1 GPa and our experiments started at 0.13 GPa [50]. Here, C_1 is described as pressure dependent: $\mathrm{C}_1^P=\mathrm{C}_1^0+\mathrm{C}_1(P)$. In one hand, Eq. (1) becomes

$$\begin{aligned}\omega_{\mathrm{LCC}}(P)&=\sqrt{\frac{2[\mathrm{C}_1^P+\mathrm{C}_3^0]}{m}}\\&=\sqrt{\frac{2\{[\mathrm{C}_1^0+\mathrm{C}_1(P)]+\mathrm{C}_3^0\}}{m}}.\end{aligned} \tag{2}$$

On the other hand, from Figs. 1(b) and 1(c) we see that $\omega_{\mathrm{LCC}}(P)$ varies linearly with pressure. Therefore,

$$\begin{aligned}\omega_{\mathrm{LCC}}(P)&=\omega_{\mathrm{LCC}}^{0}+\left(\frac{d\omega_{\mathrm{LCC}}}{dP}\right)P\\&=\omega_{\mathrm{LCC}}^{0}+\left(\frac{1}{m[\omega_{\mathrm{LCC}}(p)]}\frac{d\mathrm{C}_1}{dP}\right)P,\end{aligned} \tag{3}$$

where the slope $d\omega_{\mathrm{LCC}}/dP=\{1/m[\omega_{\mathrm{LCC}}(p)]\}d\mathrm{C}_1/dP$. Such slope gives a good approximation of how much the bond is effectively hardened or softened with P. The hydrostatic pressure applied to the MWCNTs comprises one axial component and one radial component. Since below 9 GPa the inner tubes are not expected to deform in the radial direction, it is reasonable to expect that the pressure transmitted to the LCCs comes from the axial component with increasing P [9,45–48] (see [36] for a comprehensive discussion of the model's hypotheses).

The system's restoring force ($F_{\mathrm{restoring}}$) must be proportional to the compression:

$$F_{\mathrm{restoring}}=-2[\mathrm{C}_1^P+\mathrm{C}_3^0]\Delta x, \tag{4}$$

where Δx is the average change in the bond length due to P. At equilibrium, the net force (F_{net}) must be zero. Since F_{net} is the superposition of both $F_{\mathrm{restoring}}$ and applied force (F_{applied}=PA), where $A=\pi R^2=7.8\times10^{-19}\mathrm{m}^2$ ($R=0.4$ nm is the MWCNT's innermost tube radius), we have

$$F_{\mathrm{net}}=F_{\mathrm{restoring}}+F_{\mathrm{applied}}=-2[\mathrm{C}_1^P+\mathrm{C}_3^0]\Delta x+F_{\mathrm{applied}}=0.$$

By rewriting this equation in terms of Δx we obtain

$$\Delta x=\frac{F_{\mathrm{applied}}}{2[\mathrm{C}_1^P+\mathrm{C}_3^0]}=\frac{F_{\mathrm{applied}}}{m[\omega_{\mathrm{LCC}}(P)]^2}.$$

The evaluation of the rate with which Δx changes with pressure, for each pressure and within equilibrium conditions, leads to

$$\frac{d(\Delta x)}{dP}=-\frac{2F_{\mathrm{applied}}}{m[\omega_{\mathrm{LCC}}(P)]^3}\frac{d\omega_{\mathrm{LCC}}}{dP} \tag{5}$$

We can now use Eq. (5) to determine the pressure-dependent Young's modulus of elasticity, $E(P)$. In other words,

$$E(P)=a_{\mathrm{C-C}}\frac{dP}{d(\Delta x)}=-\left\{\frac{a_{\mathrm{C-C}}m[\omega_{LCC}(P)]^3}{2A\frac{d\omega_{\mathrm{LCC}}}{dP}}\right\}P^{-1}, \tag{6}$$

where $a_{\mathrm{C-C}}=1.37\times10^{-10}$ m is the average C-C distance at ambient pressure.

The nonunified behavior shown in Fig. 1(c) suggests that the LCCs possess distinct E that depend on the number of carbon atoms and, consequently, on the LCCs' lengths. The Young's modulus is characteristic of each LCC and in the harmonic regime it must remain universal and pressure independent, contrarily to what could be expected in the anharmonic regime. The literature has reported only theoretical and pressure-independent values for E ranging from as low as 0.3 TPa to as high as 32.7 TPa [2,29,50]. Therefore, a comprehensive understanding of LCCs' E remains still an open question. Our model suggests that for a linear anharmonicity, E must be both dependent on pressure and universal for all LCCs. Universal behaviors for pressure-dependent E have been reported for other carbon systems. Barboza *et al.* [51] demonstrated that the radial Young's modulus E_r for carbon nanotubes with several distinct diameters (d_t) present a universal behavior with strain and that such dependence could be unified if E_r is multiplied by d_t^3. Using the experimental values found for $\omega_{\mathrm{LCC}}(P)$ and $d\omega_{\mathrm{LCC}}/dP$, E associated with the LCCs is obtained from Eq. (6) for different pressures. The universal and anharmonic behavior is clear from Fig. 2(a), where E for all LCCs follow a $E(P)=E_0P^{-1}$ dependence, with $E_0=-\{[a_{\mathrm{C-C}}m[\omega_{\mathrm{LCC}}(P)]^3]/[2A(d\omega_{\mathrm{LCC}}/dP)]\}$ being effectively constant, positive (note that $d\omega_{\mathrm{LCC}}/dP<0$) and distinct for each chain (see Table S1 in SM [36]).

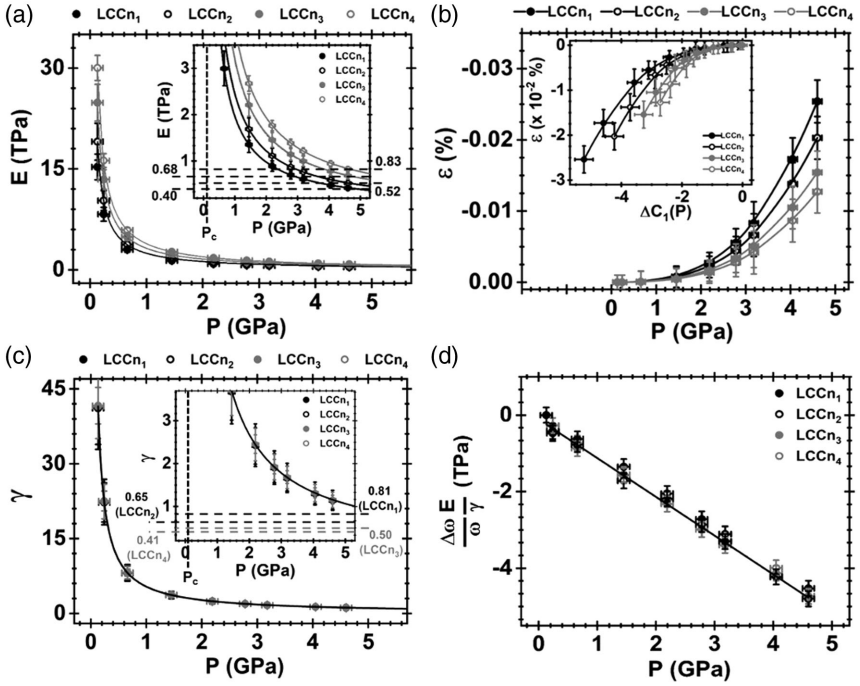

FIG. 2. (a) Young's modulus E, (b) strain ε, and (c) Grüneisen parameter γ as a function of P for each LCC. Both E and γ follow a P^{-1} universal law, while ε follows a P^2 universal law. (d) $(\Delta\omega/\omega)(E/\gamma) = -P$, an important parameter for nanometrology, is universal and unified. (a)–(d) the solid lines are experimental data fittings. Insets: (a) shows the $E(P)$ vs P graphic enlarged to highlight the $P \to \infty$ limit. The horizontal dashed lines correspond to the values E (4.60 GPa) for each LCC. (b) shows the evolution of ε with relation to the relative changes of C_1 with increasing P. (c) shows the $\gamma(P)$ vs P graphic zoomed to highlight the $P \to \infty$ limit. The horizontal dashed lines correspond to the values of γ calculated with $E = 0.3$ TPa for each LCC [50]. The vertical dashed lines in (a) and (c) stand for $P_c = 0.1$ GPa.

From Eq. (6), we obtain the LCC's hydrostatic coefficient of uniaxial strain:

$$\varepsilon(\%) = -\left\{\frac{A\frac{d\omega_{\mathrm{LCC}}}{dP}}{a_{\mathrm{C-C}}m[\omega_{\mathrm{LCC}}(P)]^3}\right\}P^2, \tag{7}$$

which is shown in Fig. 2(b). The hydrostatic coefficient of uniaxial strain is related to P by $d\varepsilon = dL/L = S \times dP$, where L is the LCC's length and the quantity $S = 1/E$ is the LCC's elastic compliance. The results in Fig. 2(b) show that longer LCCs (i.e., higher n_i, for $i = 1, \ldots, 4$) are more susceptible to higher strains with increasing pressure [36]. The inset in Fig. 2(b) shows ε as a function of $\Delta C_1(P) = C_1(P) - C_1^0$ for each LCC studied here. The dependence of $C_1(P)$ with P as well as the main steps to derive it are shown in Fig. S3 in SM [36]. The pressure-dependent Grüneisen parameter $\gamma(P)$ is obtained by considering the uniaxial effect along the LCC's length. Per definition, $\gamma(P)$ is written as [23,52,53]

$$\gamma(P) = -\frac{L}{\omega_{\mathrm{LCC}}(P)}\frac{d\omega_{\mathrm{LCC}}}{dL} = -\frac{1}{\omega_{\mathrm{LCC}}(P)}\frac{d\omega_{\mathrm{LCC}}}{d\varepsilon},$$

where $d\varepsilon = (1/L)dL = (P/E_0)dP$ and $d\omega_{\mathrm{LCC}}/d\varepsilon = (dP/d\varepsilon)(d\omega_{\mathrm{LCC}}/dP) = (E_0/P)(d\omega_{\mathrm{LCC}}/dP)$. Therefore, $\gamma(P)$ can be rewritten as

$$\gamma(P) = -\frac{E(P)}{\omega_{\mathrm{LCC}}(P)}\frac{d\omega_{\mathrm{LCC}}}{dP} = -\frac{E_0}{P\omega_{\mathrm{LCC}}(P)}\frac{d\omega_{\mathrm{LCC}}}{dP} = \left\{\frac{a_{\mathrm{C-C}}m[\omega_{\mathrm{LCC}}(p)]^2}{2A}\right\}P^{-1}. \tag{8}$$

The Grüneisen parameter $\gamma(P)$ associated with the C band follows the same trends observed for $E(P)$. In fact, Eq. (8) indicates that $\gamma(P)$ also follows the universal behavior $\gamma(P) = \gamma_0 P^{-1}$ with increasing pressure as shown in Fig. 2(c). This time, however, it is also observed that γ is unified, presenting the same $\gamma_0 = 5.36$ for every LCC. It is noteworthy that the factor $-[1/\omega_{\mathrm{LCC}}(P)](d\omega_{\mathrm{LCC}}/dP)$ multiplying $E(P)$ in Eq. (8) takes an equivalent role observed for the factor d_t^3 multiplying the radial Young's modulus E_r in the case of carbon nanotubes [51].

Figures 2(a) and 2(c) present two important limits: (1) $P \to 0$, and (2) $P \to \infty$. The first limit ($P \to 0$) says that between $P_c \le P \le \infty$, when $P \to P_c$, where P_c is the critical pressure 0.1 GPa [see insets in Figs. 2(a) and 2(c)], E increases rapidly toward values as low as 15.0 TPa (for $LCCn_1$) and as high as 30.5 TPa (for $LCCn_4$), while γ increases rapidly toward a maximum and unified value of 42. For $0 \le P \le P_c$, the LCCs are no longer in the anharmonic regime [50] and E becomes pressure independent and distinct for each LCC. Consequently, γ starts

decreasing again with $P \to 0$ assuming distinct values for each LCC (Table S1 in SM [36]). The second limit ($P \to \infty$) shows that E asymptotically converges to distinct values ranging from 0.40 TPa (for LCCn_1) to 0.83 TPa (for LCCn_4) at 4.60 GPa, while γ asymptotically converges to 1.2, as shown in the inset in Figs. 2(a) and 2(c) and summarized in Table S1 in SM [36]. Our model also stands for pressures as high as 9 GPa and it nicely explains the results by Andrade *et al.*[27] and Neves *et al.* [28] without the need of invoking mechanisms beyond the C-C single bond anharmonicity (see SM, Sec. VI and Fig. S5 [36]). The anharmonic regime provides an important perspective for LCCs' mechanical properties: Figures 2(a) and 2(c) show that hydrostatic pressures can modulate both E and γ. In one hand, γ can be tuned to assume values predicted for several other carbon structures: (1) $\gamma = 2.87$ at 1.86 GPa, expected for carbon nanofibers (G band); (2) $\gamma = 1.99$ at 2.68 GPa, expected for graphene (G band); (3) $\gamma = 1.59$ at 3.35 GPa, expected for graphite (G band); and (4) $\gamma = 1.24$ at 4.31 GPa, expected for CNTs (G band). On the other hand, E can be tuned to assume values that could be smaller, of the order, or larger than those reported for materials such as diamond (1.18–1.22 TPa), graphene (2.40 TPa), bilayer graphene (2.0 TPa) and CNTs (0.40–4.15 TPa) [6,54,55].

Another outcome from our model is shown in Fig. 2(d): the quantity $(\Delta\omega/\omega)(E/\gamma) = -P$ is also both universal and unified. Although this result is expected for pressure-independent E and γ, it is only recovered for pressure-dependent E and γ if the ratio γ/E happens to be pressure independent. Our experiment shows that LCCs of a variety of lengths (number of carbon atoms) display mechanical properties that result in a pressure-independent γ/E even though E and γ are not pressure independent [36]. This pressure-independent γ/E results from the LCCs' intrinsic properties. In other words, it is determined by the experimental values of $[\omega_{\mathrm{LCC}}(P)]^{\alpha}$ (for $\alpha = 1, 2$ and 3) and $d\omega_{\mathrm{LCC}}/dP$, and their respective ratios. Therefore, by using E and γ provided by our model along with $\Delta\omega/\omega$ provided by the Raman measurement, we suggest that LCCs can be effectively used in nanometrology for applications involving, for example, pressure calibration at the nanoscale or highly sensitive mass sensors with the advantage that one does not need to be concerned about the length distribution of LCCs to establish an efficient device. Finally, our results show that LCCs will be the strongest among the aforementioned sp^3 and sp^2 carbon materials only for $P \leq 0.6$ GPa. For $P > 0.6$ GPa the same LCCs become as strong as or even weaker than those carbon materials.

Summarizing, we studied the Raman fingerprint C band of isolated LCCs@MWCNT under hydrostatic pressures ($0.13 \leq \mathrm{P} \leq 4.60$ GPa). The dependences of ω_{LCC} with P are explained by considering the natural anharmonicity from the C-C single bond. Experimental values of $\omega_{\mathrm{LCC}}(P)$ and $d\omega_{\mathrm{LCC}}/dP$ allowed us to calculate the pressure-dependence for the LCCs' Young's modulus (E), strain (ε) and Grüneisen parameter (γ). The results show that E and γ follow universal P^{-1} laws, while ε follows a P^2 universal law. Noticeably, γ also presents a unified behavior in the range of pressures studied here. The LCCs' anharmonic behavior allows for tuning E and γ to values lower, of the order or higher than those observed for other carbon materials. The nature of LCCs' mechanical properties indicates them as effective materials for nanometrology and for the advancement of nanodevices. Our model, which considers the natural anharmonicity from the C—C single bond, explains very well other results reported in the literature [27,28]. Moreover, it has great potential to be applied in other one dimensional materials such as polymeric chains with Raman modes constrained to polymer's backbones, for example.

This material is based upon work supported by the National Science Foundation under Grant No. 1848418. P. T. A., K. S., N. M. B. N., N. L. C., and A. R. P. acknowledge both the American Physical Society (APS) and the Brazilian Physical Society (SBF, Portuguese acronym) for supporting this research through the Brazil-U.S. Ph.D. Exchange program. A. R. P. thanks Professor Paulo de Tarso Cavalcante Freire, from the Department of Physics of Universidade Federal do Ceará, Brazil, for providing the DAC high-pressure system. Y. A. K. acknowledges the financial support from the National Research Foundation of Korea (NRF) grant funded by the Korea government (MSIT) (No. NRF-2017R1A2A1A17069771). L. G. P. M. and J. K. acknowledge the support from National Science Foundation (NSF) under the EFRI2-DARE program (EFMA-1542863), from AFOSR FATE MURI, Grant No. FA9550-15-1-0514 and from CNPQ Grant No. 206251/2014-9. This work was performed in part at the Center for Nanoscale Systems (CNS), which is supported by the National Science Foundation under NSF Award No. 1541959.

*These authors contributed equally to this work.
†Corresponding author.
ptaraujo@ua.edu
‡Corresponding author.
barbosaneto@ufpa.br
§Corresponding author.
paschoal@fisica.ufc.br

[1] J. Kastner, H. Kuzmany, L. Kavan, F. Dousek, and J. Kürti, Reductive preparation of carbyne with high yield. An in situ Raman scattering study, Macromolecules **28**, 344 (1995).
[2] Y. Zhang, Y. Su, L. Wang, E. S. Kong, X. Chen, and Y. Zhang, A one-dimensional extremely covalent material: Monatomic carbon linear chain, Nanoscale Res. Lett. **6**, 577 (2011).
[3] L. Shi, P. Rohringer, K. Suenaga, Y. Niimi, J. Kotakoski, J. C. Meyer, H. Peterlik, M. Wanko, S. Cahangirov, A. Rubio, Z. J. Lapin, L. Novotny, P. Ayala, and T. Pichler,

Confined linear carbon chains as a route to bulk carbyne, Nat. Mater. **15**, 634 (2016).
[4] P. T. Araujo, Anharmonicities in phonon combinations and overtones in bilayered graphene: A temperature-dependent approach, Phys. Rev. B **97**, 205441 (2018).
[5] A. Hirsch, The era of carbon allotropes, Nat. Mater. **9**, 868 (2010).
[6] J. U. Lee, D. Yoon, and H. Cheong, Estimation of Young's modulus of graphene by Raman spectroscopy, Nano Lett. **12**, 4444 (2012).
[7] A. S. Pawbake, K. K. Mishra, L. G. B. Machuno, R. V. Gelamo, T. R. Ravindran, C. S. Rout, and D. J. Late, Temperature and pressure dependent Raman spectroscopy of plasma treated multilayer graphene nanosheets, Diam. Relat. Mater. **84**, 146 (2018).
[8] D. Yoon, Y. W. Son, and H. Cheong, Negative thermal expansion coefficient of graphene measured by Raman spectroscopy, Nano Lett. **11**, 3227 (2011).
[9] A. Aguiar, E. Barros, R. Capaz, A. Souza Filho, P. Freire, J. M. Filho, D. Machon, C. Caillier, Y. Kim, and H. Muramatsu, Pressure-induced collapse in double-walled carbon nanotubes: Chemical and mechanical screening effects, J. Phys. Chem. C **115**, 5378 (2011).
[10] J. Arvanitidis, D. Christofilos, K. Papagelis, K. Andrikopoulos, T. Takenobu, Y. Iwasa, H. Kataura, S. Ves, and G. Kourouklis, Pressure screening in the interior of primary shells in double-wall carbon nanotubes, Phys. Rev. B **71**, 125404 (2005).
[11] S. Reich, H. Jantoljak, and C. Thomsen, Shear strain in carbon nanotubes under hydrostatic pressure, Phys. Rev. B **61**, R13389 (2000).
[12] N. Bonini, M. Lazzeri, N. Marzari, and F. Mauri, Phonon Anharmonicities in Graphite and Graphene, Phys. Rev. Lett. **99**, 176802 (2007).
[13] V. I. Kasatochkin, A. M. Sladkov, Yu. P. Kudryavtsev, N. M. Popov, and V. V. Korshak, Crystalline forms of linear modification of carbon, Dokl. Akad. Nauk SSSR **177**, 358 (1967).
[14] H. W. Kroto, J. R. Heath, S. C. O'Brien, R. F. Curl, and R. E. Smalley, C60: Buckminsterfullerene, Nature (London) **318**, 162 (1985).
[15] F. Diederich and M. Kivala, All carbon scaffolds by rational design, Adv. Mater. **22**, 803 (2010).
[16] P. Smith and P. R. Buseck, Carbyne forms of carbon: Do they exist?, Science **216**, 984 (1982).
[17] R. J. Lagow, J. J. Kampa, H.-C. Wei, S. L. Battle, J. W. Genge, D. A. Laude, C. J. Harper, R. Bau, R. C. Stevens, and J. F. Haw, Synthesis of linear acetylenic carbon: the "sp" carbon allotrope, Science **267**, 362 (1995).
[18] X. Zhao, Y. Ando, Y. Liu, M. Jinno, and T. Suzuki, Carbon Nanowire made of a Long Linear Carbon Chain Inserted Inside a Multiwalled Carbon Nanotube, Phys. Rev. Lett. **90**, 187401 (2003).
[19] C. Zhao, R. Kitaura, H. Hara, S. Irle, and H. Shinohara, Growth of linear carbon chains inside thin double-wall carbon nanotubes, J. Phys. Chem. C **115**, 13166 (2011).
[20] Z. Wang, X. Ke, Z. Zhu, F. Zhang, M. Ruan, and J. Yang, Carbon-atom chain formation in the core of nanotubes, Phys. Rev. B **61**, R2472 (2000).
[21] D. Nishide, H. Dohi, T. Wakabayashi, E. Nishibori, S. Aoyagi, M. Ishida, S. Kikuchi, R. Kitaura, T. Sugai, and M. Sakata, Single-wall carbon nanotubes encaging linear chain $C_{10}H_2$ polyyne molecules inside, Chem. Phys. Lett. **428**, 356 (2006).
[22] L. Shi, P. Rohringer, M. Wanko, A. Rubio, S. Waßerroth, S. Reich, S. Cambré, W. Wenseleers, P. Ayala, and T. Pichler, Electronic band gaps of confined linear carbon chains ranging from polyyne to carbyne, Phys. Rev. Mater. **1**, 075601 (2017).
[23] J. E. Proctor, E. Gregoryanz, K. S. Novoselov, M. Lotya, J. N. Coleman, and M. P. Halsall, High-pressure Raman spectroscopy of graphene, Phys. Rev. B **80**, 073408 (2009).
[24] R. S. Alencar, W. Cui, A. C. Torres-Dias, T. F. T. Cerqueira, S. Botti, M. A. L. Marques, O. P. Ferreira, C. Laurent, A. Weibel, D. Machon, D. J. Dunstan, A. G. Souza Filho, and A. San-Miguel, Pressure-induced radial collapse in few-wall carbon nanotubes: A combined theoretical and experimental study, Carbon **125**, 429 (2017).
[25] L. Alvarez, J. L. Bantignies, R. Le Parc, R. Aznar, J. L. Sauvajol, A. Merlen, D. Machon, and A. San Miguel, High-pressure behavior of polyiodides confined into single-walled carbon nanotubes: A Raman study, Phys. Rev. B **82**, 205403 (2010).
[26] J. Sandler, M. S. P. Shaffer, A. H. Windle, M. P. Halsall, M. A. Montes-Morán, C. A. Cooper, and R. J. Young, Variations in the Raman peak shift as a function of hydrostatic pressure for various carbon nanostructures: A simple geometric effect, Phys. Rev. B **67**, 035417 (2003).
[27] N. F. Andrade, A. L. Aguiar, Y. A. Kim, M. Endo, P. T. C. Freire, G. Brunetto, D. S. Galvão, M. S. Dresselhaus, and A. G. Souza Filho, Linear carbon chains under high-pressure cnditions, J. Phys. Chem. C **119**, 10669 (2015).
[28] W. Q. Neves, R. S. Alencar, R. S. Ferreira, A. C. Torres-Dias, N. F. Andrade, A. San-Miguel, Y. A. Kim, M. Endo, D. W. Kim, H. Muramatsu, A. L. Aguiar, and A. G. Souza Filho, Effects of pressure on the structural and electronic properties of linear carbon chains encapsulated in double wall carbon nanotubes, Carbon **133**, 446 (2018).
[29] M. Liu, V. I. Artyukhov, H. Lee, F. Xu, and B. I. Yakobson, Carbyne from first principles: Chain of C atoms, a nanorod or a nanorope, ACS Nano **7**, 10075 (2013).
[30] A. K. Nair, S. W. Cranford, and M. J. Buehler, The minimal nanowire: Mechanical properties of carbyne, Europhys. Lett. **95**, 16002 (2011).
[31] F. Cataldo, *Polyynes: Synthesis, Properties, and Applications* (CRC Press, Boca Raton, 2005).
[32] M. Wang and S. Lin, Ballistic thermal transport in carbyne and cumulene with micron-scale spectral acoustic phonon mean free path, Sci. Rep. **5**, 18122 (2016).
[33] O. Cretu, A. R. Botello-Mendez, I. Janowska, C. Pham-Huu, J.-C. Charlier, and F. Banhart, Electrical transport measured in atomic carbon chains, Nano Lett. **13**, 3487 (2013).
[34] R. B. Heimann, S. E. Evsyukov, and L. Kavan, *Carbyne and Carbynoid Structures* (Springer, Netherlands, 1999), Vol. 21.
[35] C. Z. Wang, C. T. Chan, and K. M. Ho, Tight-binding molecular-dynamics study of phonon anharmonic effects in silicon and diamond, Phys. Rev. B **42**, 11276 (1990).
[36] See Supplemental Material at http://link.aps.org/supplemental/10.1103/PhysRevLett.125.105501 for comprehensive

discussions on the theoretical model and experimental methods and additional figures and a table that contribute with the understanding of the Letter, which includes Ref. [37].

[37] K. Matsuda, Y. Maniwa, and H. Kataura, Highly rotational C_{60} dynamics inside single-walled carbon nanotubes: NMR observations, Phys. Rev. B **77**, 075421 (2008).

[38] C. S. Kang, K. Fujisawa, Y. I. Ko, H. Muramatsu, T. Hayashi, M. Endo, H. J. Kim, D. Lim, J. H. Kim, and Y. C. Jung, Linear carbon chains inside multi-walled carbon nanotubes: Growth mechanism, thermal stability and electrical properties, Carbon **107**, 217 (2016).

[39] L. G. P. Martins, D. L. Silva, J. S. Smith, A.-Y. Lu, C. Su, M. Hempel, C. Occhialini, X. Ji, R. Pablo, and R. S. Alencar, Evidence for a pressure-induced phase transition of few-layer graphene to 2D diamond, arXiv:1910.01591.

[40] N. Andrade, T. Vasconcelos, C. Gouvea, B. Archanjo, C. Achete, Y. Kim, M. Endo, C. Fantini, M. Dresselhaus, and A. Souza Filho, Linear carbon chains encapsulated in multiwall carbon nanotubes: Resonance Raman spectroscopy and transmission electron microscopy studies, Carbon **90**, 172 (2015).

[41] H. Mao, J. A. Xu, and P. Bell, Calibration of the ruby pressure gauge to 800 kbar under quasi hydrostatic conditions, J. Geophys. Res. **91**, 4673 (1986).

[42] J. Li, C. Papadopoulos, J. Xu, and M. Moskovits, Highly-ordered carbon nanotube arrays for electronics applications, Appl. Phys. Lett. **75**, 367 (1999).

[43] A. Aqel, K. M. A. El-Nour, R. A. Ammar, and A. Al-Warthan, Carbon nanotubes, science and technology part (I) structure, synthesis and characterization, Arab. J. Chem. **5**, 1 (2012).

[44] M. M. Haque, L. Yin, A. R. Nugraha, and R. Saito, Vibrational and NMR properties of polyynes, Carbon **49**, 3340 (2011).

[45] R. Alencar, A. Aguiar, A. Paschoal, P. Freire, Y. Kim, H. Muramatsu, M. Endo, H. Terrones, M. Terrones, and A. San-Miguel, Pressure-induced selectivity for probing inner tubes in double-and triple-walled carbon nanotubes: A resonance Raman study, J. Phys. Chem. C **118**, 8153 (2014).

[46] S. D. Silva-Santos, R. S. Alencar, A. L. Aguiar, Y. A. Kim, H. Muramatsu, M. Endo, N. P. Blanchard, A. San-Miguel, and A. G. Souza Filho, From high pressure radial collapse to graphene ribbon formation in triple-wall carbon nanotubes, Carbon **141**, 568 (2019).

[47] M. Chorro, S. Rols, J. Cambedouzou, L. Alvarez, R. Almairac, J.-L. Sauvajol, J.-L. Hodeau, L. Marques, M. Mezouar, and H. Kataura, Structural properties of carbon peapods under extreme conditions studied using in situ x-ray diffraction, Phys. Rev. B **74**, 205425 (2006).

[48] S. Rols, J. Cambedouzou, M. Chorro, H. Schober, V. Agafonov, P. Launois, V. Davydov, A. Rakhmanina, H. Kataura, and J.-L. Sauvajol, How Confinement Affects the Dynamics of C_{60} in Carbon Nanopeapods, Phys. Rev. Lett. **101**, 065507 (2008).

[49] G. Dereli and C. Özdoğan, Structural stability and energetics of single-walled carbon nanotubes under uniaxial strain, Phys. Rev. B **67**, 035416 (2003).

[50] S. Kotrechko, I. Mikhailovskij, T. Mazilova, E. Sadanov, A. Timoshevskii, N. Stetsenko, and Y. Matviychuk, Mechanical properties of carbyne: Experiment and simulations, Nanoscale Res. Lett. **10**, 24 (2015).

[51] A. Barboza, H. Chacham, and B. Neves, Universal Response of Single-Wall Carbon Nanotubes to Radial Compression, Phys. Rev. Lett. **102**, 025501 (2009).

[52] C. Kittel, *Introduction to Solid State Physics* (Wiley New York, 1976), Vol. 8.

[53] T. M. G. Mohiuddin, A. Lombardo, R. R. Nair, A. Bonetti, G. Savini, R. Jalil, N. Bonini, D. M. Basko, C. Galiotis, N. Marzari, K. S. Novoselov, A. K. Geim, and A. C. Ferrari, Uniaxial strain in graphene by Raman spectroscopy: *G* peak splitting, Grüneisen parameters, and sample orientation, Phys. Rev. B **79**, 205433 (2009).

[54] C. A. Klein and G. F. Cardinale, Young's modulus and Poisson's ratio of CVD diamond, Diam. Relat. Mater. **2**, 918 (1993).

[55] M. J. Treacy, T. Ebbesen, and J. Gibson, Exceptionally high Young's modulus observed for individual carbon nanotubes, Nature (London) **381**, 678 (1996).